Drying Technology
An International Journal

ISSN: 0737-3937 (Print) 1532-2300 (Online) Journal homepage: http://www.tandfonline.com/loi/ldrt20

Modeling of Combined Microwave and Convective Drying of Wood: Prediction of Mechanical Behavior via Internal Gas Pressure

Sahbi Ouertani, Lamine Hassini, Soufien Azzouz, Sadoth Sandoval Torres, Ali Belghith & Ahmed Koubaa

To cite this article: Sahbi Ouertani, Lamine Hassini, Soufien Azzouz, Sadoth Sandoval Torres, Ali Belghith & Ahmed Koubaa (2015) Modeling of Combined Microwave and Convective Drying of Wood: Prediction of Mechanical Behavior via Internal Gas Pressure, Drying Technology, 33:10, 1234-1242, DOI: 10.1080/07373937.2015.1022828

To link to this article: http://dx.doi.org/10.1080/07373937.2015.1022828

Accepted author version posted online: 01 Apr 2015.
Published online: 01 Apr 2015.

Drying Technology, 33: 1234–1242, 2015

ISSN: 0737-3937 print/1532-2300 online
DOI: 10.1080/07373937.2015.1022828

Taylor & Francis
Taylor & Francis Group

Modeling of Combined Microwave and Convective Drying of Wood: Prediction of Mechanical Behavior via Internal Gas Pressure

Sahbi Ouertani,[1] Lamine Hassini,[1] Soufien Azzouz,[1] Sadoth Sandoval Torres,[2] Ali Belghith,[1] and Ahmed Koubaa[3]

[1]*Laboratoire d'Énergétique et des Transferts Thermiques et Massique, Département de Physique, Faculté des Sciences de Tunis, Université de Tunis El Manar, El Manar, Tunis, Tunisia*
[2]*Instituto Politécnico Nacional, CIIDIR-Oaxaca, Col. Noche Buena, Santa Cruz Xoxocotlan, Oaxaca, Mexico*
[3]*Chaire de Recherche du Canada sur la Valorisation, la Caractérisation et la Transformation du bois, Université du Québec en Abitibi-Témiscamingue, Rouyn-Noranda, Québec, Canada*

The impact of microwave drying on the quality of dried wood remains unclear. Particular attention should be paid in order to optimize the combined microwave and convective drying process. In this study, a comprehensive internal heat and mass transfer model was developed and numerically implemented in order to simulate and understand the physical phenomena occurring inside Jack pine wood during a combined microwave and convective drying process. The model was validated on the basis of the average moisture content curves for drying scenarios at various microwave power levels. According to the simulations results, an increase in microwave power significantly decreases the drying time of Jack pine wood and increases its internal gas pressure, which increases the risk of cracking. However, compared to purely conventional convective drying, combined microwave and convective drying at medium microwave power and air temperature significantly reduces the drying time and maintains the internal gas pressure at reasonable values. At these conditions, the risk of cracking will be diminished. This last result was checked via experimental measurements of the sample strength dried at different microwave power levels. From this study, we can consider that for Jack pine wood, combined microwave and convective drying is a more efficient technology compared to classical convective drying.

Keywords Combined microwave and convective drying; Internal gas pressure; Jack pine wood; Modeling and simulation; Strength

Correspondence: Sahbi Ouertani, Laboratoire d'Énergétique et des Transferts Thermiques et Massique, Département de Physique, Faculté des Sciences de Tunis, Université de Tunis El Manar, Campus Universitaire, 2092 El Manar, Tunis, Tunisia; E-mail: Sahbi.Ouertani@uqat.ca

Color versions of one or more of the figures in the article can be found online at www.tandfonline.com/ldrt.

INTRODUCTION

Microwave energy is employed in some important industrial sectors, such as wood, food, and rubber industries, and is considered more efficient in terms of drying times compared to the conventional convective process.[1–4] However, the use of microwave energy in the wood industry to dry lumber is limited. This could be attributed to insufficient knowledge of the complex interactions between solid material, depth penetration, and process parameters during heating.[5] The majority of technically dried timber is processed in conventional heat and vent kilns. Conventional drying of wood is a slow, time-consuming, and costly process.[6] For that reason, interest is oriented to study the electroheating technology of wood, in particular, microwave energy for specific applications in the wood industry to achieve specific objectives, such as reducing the drying time and energy consumption and providing better mechanical properties with high strength than conventional processes.[6,7] Commercialization of wood heating processes is of growing interest for its potential use in pasteurization of wood to eradicate exotic pest infestations in lumber.[3,8] This technology is able to pasteurize the wood pallets and crates or other forms of solid wood packing materials for international exchange.[9] It has been approved by the U.N. Phytosanitary Commission[10] and the U.S. Department of Agriculture[11] as sanitization treatment for wood packing materials. Several studies demonstrated the advantage of combined microwave and convective heating on the drying performance of a large variety of materials, such as individual wood boards.[7,11–17] This technology offers a better heat transfer to the product having a lower thermal conductivity in comparison with convective or contact heating processes. Indeed, for microwave heating, the heat is generated in the product and dissipated mainly in the wet region.[7,15–18]

Mathematical modeling is an essential tool that facilitates the understanding of the physical phenomena occurring in the product during microwave drying and process optimization.[19] The modeling of combined microwave and convective drying has been attempted in order to understand the Jack pine wood–microwave interaction. Nevertheless, a comprehensive approach must be implemented because moisture transport in wood is a multimechanistic process. The static bending strength of dried wood was compared to the internal gas pressure to predict the mechanical states of end product, which can assist in optimizing the Jack pine drying parameters.

During microwave drying, moisture transport within wood can be driven by diffusion, capillarity, and internal gas pressure gradients as a result of volumetric heating. The temperature increases and passes through the boiling point of water and the resultant intense internal gas pressure pushes the water within and out of the product quickly and efficiently under the action of pumping phenomenon.[15,20,21]

During drying, moisture, temperature, and gas pressure gradients involve product shrinkage and then development of strain and stress fields inside the wood board.[22] To our knowledge, few published works concerning the impact of microwave heating on the mechanical behavior of dried wood[23] and no information about Jack pine wood has been published.

The goal of the present work was to simulate in one dimension the spatiotemporal evolution of the moisture content, temperature, and gas pressure within Jack pine wood samples during combined microwave and convective drying and to predict the mechanical state of dried wood samples via internal gas pressure in order to optimize the processing parameters.

MATERIALS AND EXPERIMENTAL PROCEDURES

The drying experiments were performed using a laboratory microwave oven (Fig. 1) with a maximum power output of 1,000 W at 2,450 MHz frequency, with a working cavity of $370 \times 350 \times 206\,\text{mm}^3$, relative humidity ranging from 10 to 90% without condensation, and air velocity about 0.5 m/s. The microwave source is placed on top of the drying chamber. Air flow and vapor evacuation were performed using a ventilator. For each experiment, one Jack pine (*Pinus banksiana*) lumber piece at the green state of 150 mm length, 100 mm width, and 12 mm thick were used. The samples were cut from lumber pieces randomly sampled in the mill yard of Tembec's Sawmill in La Sarre, Québec, Canada. During the drying process, the wood samples were placed at the center of the drying chamber and removed periodically to measure its instantaneous mass. The product moisture content in the dry basis was calculated according to the following relationship:

$$\mathrm{M}\,(\%) = \frac{\mathrm{W} - \mathrm{W_d}}{\mathrm{W_d}} \times 100 = \frac{\mathrm{W_{water}}}{\mathrm{W_d}} \times\ 100. \qquad (1)$$

The moisture content ratio was given by the following equation:

$$\mathrm{MR} = \frac{\mathrm{M}}{\mathrm{M_{ini}}}, \qquad (2)$$

where M is the average moisture content (kg water/kg DM), W is the wood sample mass (kg), W_{water} is the water mass (kg), W_{d} is the oven dry mass (kg), and M_{ini} is the initial moisture content (kg water/kg DM).

According to Ouertani et al.,[24] the wood dry mass was obtained after keeping the samples in a controlled-temperature oven at $103 \pm 2^{\circ}\text{C}$ until a constant mass was reached.

The bending strength and the Young's modulus of dried wood samples (dimensions $20 \times 20 \times 300\,\text{mm}^3$) were determined according to ASTM D143[25] using a universal testing machine (Zwick Roell Z20, Germany). The protocol specified for sample sawing is modified with regard to the microwave oven dimensions. The wood specimens selected for the mechanical tests were conditioned in a controlled environment room at a temperature of 20°C and a relative humidity of 50% until reaching an equilibrium target moisture content of 9%. The actual moisture content of the wood after testing ranged from 9 to 12%.

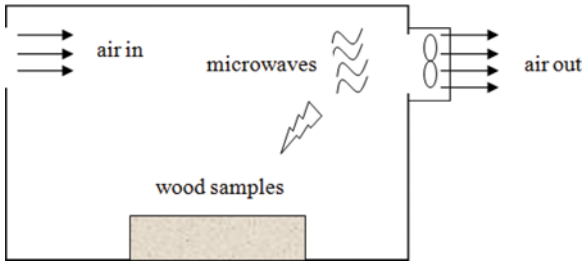

FIG. 1. Layout of the laboratory microwave dryer (BP 111).

HEAT AND MASS TRANSFER MODEL

The mathematical model used in this article to describe the physical phenomena involved in hygroscopic capillary porous medium subjected to combined microwave and convective drying was based on the macroscopic approach of Whitaker.[26] The internal heat and mass transfer model was developed mainly on the basis of reports published by Hassini et al.,[15] Constant et al.,[16] and Perré and Turner.[20,21] It consists of four partial differential equations (Eqs. (3)–(7)). The formulation of transfer equation and assumptions were detailed in the literature.[7,12–16,26–33]

The volumetric thermal power dissipated within the product was established as a semi-empirical correlation.[5,12]

System of Equations

The liquid water transfer equation determining the moisture content M is obtained by summation of the conservation equations of vapor (v), free water (l), and bound water (b) and written as follows[13,15,29,30]:

$$\frac{\partial \mathrm{M}}{\partial \mathrm{t}} = -\nabla\left\{\frac{1}{\overline{\rho_s}}\left[\left(\mathrm{D_l^M} + \mathrm{D_b^M} + \mathrm{D_v^M}\right)\nabla \mathrm{M} + \left(\mathrm{D_l^T} + \mathrm{D_v^T}\right)\nabla \mathrm{T} + \left(\mathrm{D_l^P} + \mathrm{D_v^P}\right)\nabla \mathrm{P}_g\right]\right\} \quad (3)$$

The equation for the total pressure of the gaseous phase P_g is obtained from the readings of the mass balance on dry air[13,15]:

$$\gamma_1 \frac{\partial \mathrm{P_g}}{\partial \mathrm{t}} + \gamma_2 \frac{\partial \mathrm{M}}{\partial \mathrm{t}} + \gamma_3 \frac{\partial \mathrm{T}}{\partial \mathrm{t}} = -\nabla\left[\mathrm{D_a^M}\nabla \mathrm{M} + \mathrm{D_a^T}\nabla \mathrm{T} + \mathrm{D_a^P}\nabla \mathrm{P_g}\right] \quad (4)$$

The energy conservation equation on temperature T is written as follows[29,30]:

$$\overline{\rho \mathrm{C_p}}\frac{\partial \mathrm{T}}{\partial \mathrm{t}} + \Delta \mathrm{H_v}\left(\dot{\mathrm{m}} + \dot{\mathrm{m}}_\mathrm{b}\right) - \rho_\mathrm{s}.\mathrm{H_{sorp}}.\frac{\partial \mathrm{M_b}}{\partial \mathrm{t}} + \sum_i \rho_\mathrm{i} \mathrm{v_i} \mathrm{c_{pi}} \nabla \mathrm{T} - \nabla(\lambda \nabla \mathrm{T}) = s \quad (5)$$

The water vapor transfer equation determining the mass of liquid water vaporized per unit volume (m_{vap}) is given by the following equation[15]:

$$\frac{\partial \mathrm{m_{vap}}}{\partial \mathrm{t}} = \nabla\left[\mathrm{D_v^M}\nabla \mathrm{M} + \mathrm{D_v^T}\nabla \mathrm{T} + \mathrm{D_v^P}\nabla \mathrm{P_g}\right]. \quad (6)$$

The general structure of the model can be presented in the following way[15]:

$$[\mathrm{A}]\begin{bmatrix} \frac{\partial \mathrm{T}}{\partial \mathrm{t}} \\ \frac{\partial \mathrm{M}}{\partial \mathrm{t}} \\ \frac{\partial \mathrm{P_g}}{\partial \mathrm{t}} \\ \frac{\partial \mathrm{m_{vap}}}{\partial \mathrm{t}} \end{bmatrix} = \mathrm{div}\left\{[\mathrm{K}]\begin{bmatrix} \mathrm{gradT} \\ \mathrm{gradM} \\ \mathrm{gradP_g} \end{bmatrix}\right\} + s,$$

where [A] is the capacity matrix, [K] is the conductance matrix, and [s] is the source term, which is used only for the heat transfer equation and accounts for the heat generated within the wood by dissipation of microwave energy. The term $\frac{\partial \mathrm{m_{vap}}}{\partial \mathrm{t}}$ represents the liquid to vapor phase change rate term.

Microwave Power Source Term

Microwave power absorption by the wood samples during drying is given by the semi-empirical relation[5,12]

$$\Phi = \Phi_i \frac{\varepsilon''(\mathrm{M})}{\varepsilon_i''}, \quad (7)$$

where Φ_i represents the absorbed microwave power at the beginning of the microwave drying test, ε_i'' is the loss factor corresponding to initial moisture content, and $\varepsilon''(M)$ is the loss factor versus moisture content. The correlation of $\varepsilon''(M)$ used in this work was that for wood species, measured and published by Koubaa et al.[3]

Boundary Conditions

The water balance equation at the product surface ($x = e$ and $x = 0$) was written in the following way[7,29,30]:

$$\left(\overline{\rho_l \mathrm{V_l}} + \overline{\rho_b \mathrm{V_b}} + \overline{\rho_v \mathrm{V_v}}\right).\mathrm{n} = \mathrm{h_m c\, M_v}\frac{2.2}{2.2 - \mathrm{x_{vsurf}} - \mathrm{x_{va}}}\left(\mathrm{x_{vsurf}} - \mathrm{x_{va}}\right), \quad (8)$$

where

$$\mathrm{c} = \frac{\mathrm{P_{atm}}}{\mathrm{RT_a}}, x_\mathrm{v} = \frac{\mathrm{P_v M_v}}{(\mathrm{P_g} - \mathrm{P_v})\mathrm{M_a} + \mathrm{M_a M_v}}. \quad (9)$$

The heat balance equation at the surface ($x = e$ and $x = 0$) was written in the following way:

$$\left[\lambda \nabla \mathrm{T} + \overline{\rho_b \mathrm{V_b}}\,\mathrm{H_{sorp}} + \Delta \mathrm{h_v}\left(\overline{\rho_l \mathrm{V_l}} + \overline{\rho_b \mathrm{V_b}}\right)\right].\mathrm{n} = \mathrm{h}(\mathrm{T_a} - \mathrm{T_{surf}}) \quad (10)$$

The pressure at sample surface is considered equal to the atmospheric pressure:

$$P_g = P_{atm}. \quad (11)$$

The equations of our model were solved numerically using COMSOL Multiphysics software (3.5.a) and with the open PDE coefficient form mode. The direct (UMFPACK) linear solver system was used.[15,33] The thermophysical wood properties used in the simulation are detailed in Appendix B.

RESULTS AND DISCUSSION

Model Validation

In order to test the predictions of the model, comparisons were made with the experimental and numerical works of Perré and Turner[21] and Turner et al.[7] for purely convective and combined microwave and convective drying of softwood board, respectively. As can be seen, very reasonable agreement is obtained with the average

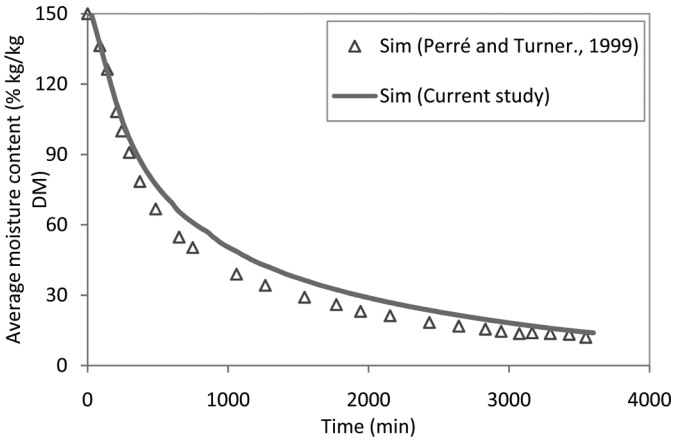

FIG. 2. Comparison of our simulated results with those of Perré and Turner[21] in the case of purely convective drying.

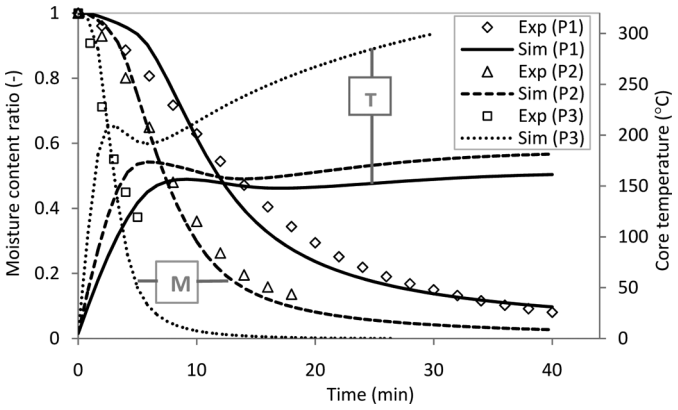

FIG. 4. Core temperature (simulated) and mean moisture content (measured and simulated) versus time for different drying conditions.

moisture contents for purely convective (Fig. 2) and combined microwave convective (Fig. 3) drying. The slight misfit (maximum relative difference of 15%) observed could be attributed to the modification of the microstructure of wood treated with intense microwave energy and the complex dielectric behavior, which depends on species, temperature, and moisture content of the wood.[3] At the end of the drying operation, the product is already totally dry and our semi-empirical expression representing the microwave energy dissipated within the product was not accurate for very low water content.[15] In order to emphasize its potential, our model was applied to thin Jack pine wood samples (12 mm × 100 mm × 150 mm) during combined microwave and convective dying. The simulation was carried out along the thickness in the tangential direction of the wood sample. Our model correctly describes the evolution of the average moisture content of the material all over the combined microwave and convective drying process (Fig. 4). The model could then be considered valid and able to predict the hydrothermal state of Jack pine wood. The operating parameters for each drying test are given in Table 1.

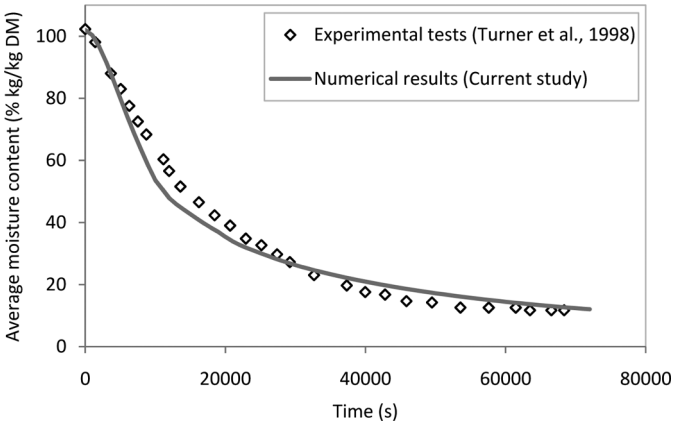

FIG. 3. Validation of the model on the basis of previous combined microwave and convective drying work.

Exploratory Simulations

Figures 4 and 5 show that, for all operating drying conditions (Table 1), an increase in microwave power decreases the drying time and increases both the core temperature and the internal gas pressure. Fundamentally, the increase in electromagnetic field level generates an important excitation of polar molecules. Then, the molecular agitation causes an intermolecular chock accompanied by important heating of product.[12] With internal heat generation, in microwave and dielectric systems, mass transfer is primarily due to the total pressure gradient established because of the rapid vapor generation within the material.[34]

Typical curves describing three successive periods of temporal evolution of core temperature, average moisture content, and internal gas pressure during microwave drying are shown in Figs. 4 and 5. At the beginning of microwave heating, a warm-up period takes place. It is characterized by quick rising temperatures, without significant mass losses and unchanged pressure (equal to atmospheric pressure). The second period is the evaporation period, characterized by the majority evaporation of moisture

TABLE 1
Operating drying conditions for model validation

Drying conditions	Incident power level (W)	T_a (°C)	Relative humidity (%)	V_a (m/s)
P1	300	30	40	0.5
P2	400	30	40	0.5
P3	1,000	30	40	0.5
P4	0	60	10	0.5

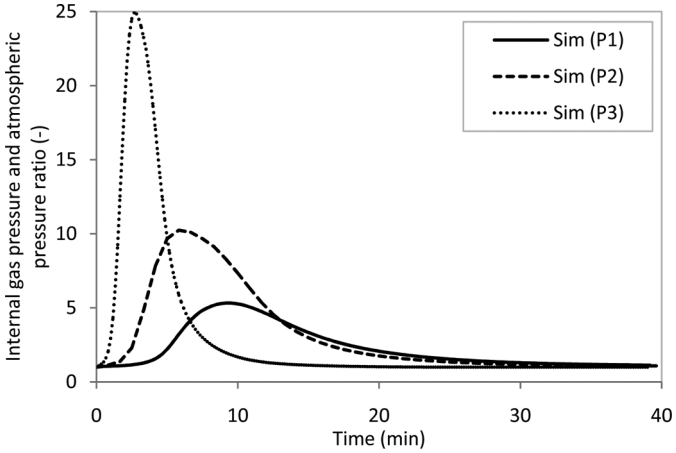

FIG. 5. Internal gas pressure and atmospheric pressure ratio versus time at different drying conditions.

content due to the important overpressure inside the medium. The third period, or the heating up period, takes place at the end of drying operation. This period is characterized by a slow evaporation of moisture content and a fast increase in temperature inside the wood under high microwave power (P3) and more slowly under low microwave level (P1 and P2). The increase in temperature is due to excessive heat built up inside the wood sample. A similar trend was founded by Du et al.[35] for wood strands and Constant et al.[16] for light concrete.

Effect of Initial Moisture Content on the Drying Kinetics

The impact of the initial wood moisture content on the drying kinetics is shown in Fig. 6. It can be seen that the decrease in initial moisture content decreases the drying time and the internal gas pressure. The reason is that high moisture content always absorbs more microwave energy, appear fast warm-up period and fast moisture evaporating.[36] As the moisture content of the sample decreases, the permeability increases and the pressure at all locations within the sample decreases.[34] Microwave treatment generates a modification of the wood structure and reveals a dramatic increase in wood permeability.[36]

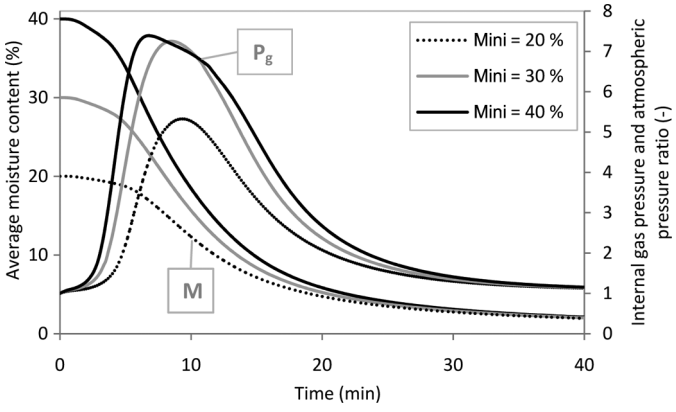

FIG. 6. Mean moisture content and internal gas phase pressure versus time at different initial moisture contents and under drying conditions of P1.

Moisture Content, Temperature, and Gas Pressure Profiles Along the Sample Thickness

Figures 7–9 show the moisture content, temperature, and gas-phase pressure profiles along the Jack pine sample thickness during combined microwave and convective drying. At the beginning of the process, moisture migration took place only at the sample's surface. The core moisture remained unchanged for about 3 min of drying. Similarly, slight increases in pressure and temperature within the sample are shown. As the drying proceeds, the moisture migration within the sample becomes most important at its surface. The internal heat generation due to microwave heating results in internal pressure and temperature buildup, which facilitate the pressure-driven moisture migration under the action of pumping phenomenon (Figs. 8 and 9). It is interesting to note the significant temperature and gas pressure gradients between the core and the surface of Jack pine wood sample. The core region affected by the temperature and the gas pressure presents the lowest moisture content and vice versa.

The simulated temperature and gas pressure profiles along the sample thickness, shown in Figs. 8 and 9, demonstrated that the highest pressure and temperature within the wood sample occur at the center of the sample. A similar parabolic shape of moisture, pressure, and temperature were found in previous reports for some hygroscopic products.[7,12,16,29,30]

Impact of Microwave Power Level on the Mechanical Properties of Dried Wood

This part of the study evaluates the impact of drying method on the strength of dried wood samples. Table 2

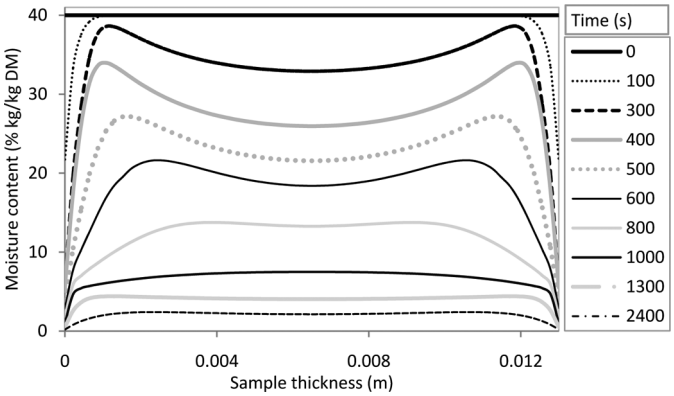

FIG. 7. Moisture content profile during microwave heating under drying conditions of P1.

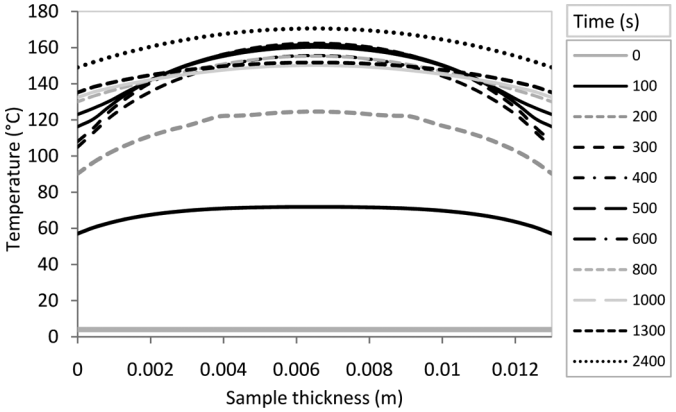

FIG. 8. Temperature profile during microwave heating under drying conditions of P1.

shows the results of static bending tests and the internal gas pressure and atmospheric pressure ratio of dried timber according to drying method. The results show that an increase in microwave power level decreases the drying time and internal gas overpressure and reduces the strength of the dried timber. The dried samples in a conventional oven at low temperature ($T = 60°C$, relative humidity = 10%) present the best mechanical properties and low internal gas overpressure compared to combined ambient convective and microwave heating. Analysis of the mechanical properties data obtained in the current experiments reveals that the microwave-dried wood samples present the lowest strength values, and the highest values were obtained by the conventional oven at low temperature. Similar results were obtained by Oloyede and Groombridge[23] for Caribbean pine wood. The experimental data in terms of mechanical strength and numerical results in terms of internal gas pressure allow optimizing the drying conditions of combined microwave and convective drying of wood. It can be concluded that the internal gas pressure buildup generates deterioration inside the wood samples and reduces its mechanical strength by comparing failure strength data with the load applied in the tangential direction and internal gas pressure shown in Table 2.

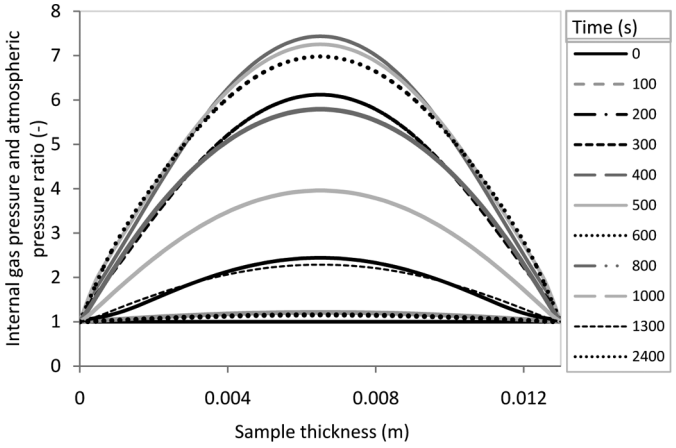

FIG. 9. Pressure profile during microwave heating under drying conditions of P1.

TABLE 2
Effect of microwave power level on wood static bending strength

Drying method	Drying time (min)	Failure strength (MPa)	Core (P/P_{atm})	Modulus of elasticity (GPa)
P1	40	64.51 ($\sigma = 11.38$)	5.3	6.422 ($\sigma = 1.882$)
P2	20	63.14 ($\sigma = 14.96$)	10.2	6.830 ($\sigma = 2.709$)
P3	5	50.56 ($\sigma = 14.49$)	25	5.1262 ($\sigma = 1.144$)
P4	2400	70.66 ($\sigma = 6.37$)	1.005	6.2122 ($\sigma = 1.144$)

σ = standard deviation.

Optimization of the drying process consists of predicting the product state evolution for different combined microwave and convective drying schedules and finding the best operating conditions to ensure fast water removal with no material cracking. The product damage risks during drying were due to the moisture content gradient and anisotropic shrinkage below the fiber saturation point and depend greatly on gas-phase (vapor and air) overpressure inside the sample.[36]

CONCLUSIONS

Numerical simulation results and experimental data were compared in this study to optimize the combined microwave and convective drying conditions of Jack pine wood. The comprehensive heat and mass transfer model was elaborated to predict the moisture content migration, temperature, and internal gas pressure during drying of the product. The model validation was established for two drying cases: convective and combined convective and microwave drying. The results demonstrated that the microwave heating of wood shortens the drying time but reduces the mechanical properties of the dried product compared to conventional air drying only at low temperature. The solution to the compromise of faster drying and mechanical quality of the dried product consists of following the drying schedule by alternating the microwave power and convective drying parameters in order to diminish the internal overpressure buildup inside the medium. Faster drying time and good quality of the dried end-product is beneficial for the wood industry.

Future work will be concentrated on modeling and simulating wood drying by considering material variability (anisotropy of shrinkage/swelling, stiffness and strength anisotropy, anisotropy of permeability and diffusivity, etc.).

NOMENCLATURE

a_w	Water activity
Cp	Specific heat (J/(kg. K))
C_{pa}	Specific heat of air (J/(kg. K))
C_{pl}	Specific heat of liquid water (J/(kg. K))
C_{ps}	Specific heat of product (J/(kg. K))
D_b	Bound water diffusion coefficient (m^2/s)
D_{eff}	Effective diffusivity (m^2/s)
$D_a^{j=M,T,P}$	Coefficient of air dry fluxes
$D_l^{j=M,T,P}$	Coefficient of liquid fluxes
$D_v^{j=M,T,P}$	Coefficient of vapor fluxes
e	Sample thickness (mm)
H_{sorp}	Heat of desorption (J/kg)
ΔH_v	Latent heat of vaporization (J/kg)
h	Convective heat transfer coefficient at the product surface ($W/(m^2\,K)$)
h_m	Mass transfer coefficient at the product surface (m/s)
K_g	Gas permeability (m^2)
K_l	Liquid permeability (m^2)
K_{rg}	Relative gas permeability
K_{rl}	Relative liquid permeability
M	Wood moisture content (kg/(kg. DM))
M_a	Air molar mass (kg/mol)
M_g	Gas molar mass (kg/mol)
MR	Moisture ratio
$\dot{m}$	Rate of evaporation ($kg/m^3.s$)
P_{atm}	Atmospheric pressure (Pa)
P_c	Cappillary pressure (Pa)
P_g	Gaseous pressure (Pa)
P_v	Water vapor pressure within the product (Pa)
R	Ideal gas constant (J/mol. K)
RH	Relative humidity (%)
S	Saturation
s	Source term
T	Wood temperature (°C, K)
t	Time (s)
V	Velocity (m/s)
v	Speed (m/s)

Greek Symbols

ε	Porosity
ε''	Loss factor
λ	Thermal conductivity (W/(m.K))
$\gamma_1, \gamma_2, \gamma_3$	Coefficients of pressure equation
μ	Dynamic viscosity (kg/(m.s))
v	Phase volume (air or vapor)
ρ	Density (kg/m^3)
σ	Standard deviation
Φ	Volumetric thermal power dissipated by microwaves within the product (W/m^3)

Subscripts and Superscripts

a	Air
b	Bound
d	Dry
fsp	Fiber saturation point
g	Gas
i	Air or vapor phase
ini	Initial
l	Liquid water
M	Moisture content
P	Pressure
s	solid
surf	Surface
T	Tangential direction
T	Temperature
v	Water vapor

ACKNOWLEDGMENTS

Our thanks go to Gilles Villeneuve, from the University of Quebec in Abitibi-Témiscamingue, and Abderrazak Zaaraoui, from the University of Tunis El Manar, for their technical assistance and help in carrying out the experiments.

FUNDING

The first author acknowledges financial support from the Tunisian government and the Canada Research Chair for Wood Assessment, Development and Processing.

REFERENCES

1. Resch, H. *Drying Wood with High Frequency Electric Current*; Society of Wood Science and Technology: Madison, WI, 2009.
2. Resch, H. High-frequency heating combined with vacuum drying of wood. In *Proceedings of the 8th International IUFRO Wood Drying Conference*, Brasov, Romania, August 24–29, 2003.
3. Koubaa, A.; Perré, P.; Hutcheon, R.M.; Lessard, J. Complex dielectric properties of the sapwood of aspen, white birch, yellow birch, and sugar maple. *Drying Technology* **2008**, *26*, 568–578.
4. Appleton, T.J.; Colder, R.I.; Kingman, S.W.; Lowndes, I.S.; Read, A.G. Microwave technology for energy-efficient processing of waste. *Applied Energy* **2005**, *81*, 85–113.
5. Anti, A.; Perré, P. A microwave applicator for on line wood drying: Temperature and moisture distribution in wood. *Wood Science and Technology* **1999**, *33*, 123–138.
6. Vongpradubchai, S.; Rattanadecho, P. The microwave processing of wood using a continuous microwave belt drier. *Chemical Engineering and Processing* **2009**, *48*, 997–1003.
7. Turner, I.W.; Puiggali, J.R.; Jomaa, W. A numerical investigation of combined microwave and convective drying of a hygroscopic porous material. A study based on pine wood. *Chemical Engineering Research & Design* **1998**, *76*, 193–209.
8. Erchiqui, F.; Annasabi, Z.; Koubaa, A.; Kocaefe, D.; Slaoui-Hasnaoui, F.; Imad, A. Numerical investigation on phytosanitary treatment of frozen wood using microwave energy. *Canadian Journal of Chemical Engineering* **2014**, *92*, 1859–1864.

9. Fleming, M.R.; Janowiak, J.J.; Kimmel, J.D.; Halbrendt, J.M.; Bauer, L.S.; Miller, D.L.; Kelli, H. Efficacy of commercial microwave equipment for eradication of pine wood nematodes and cerambycid larvae infesting red pine. *Forest Product Journal* **2005**, *55*, 226–232.
10. United Nations. Guidelines for regulating wood packaging material in international trade. In *International Standards for Phytosanitary Measures*, Publication No. 15. Food and Agriculture Organization of the United Nations: Rome, Italy, 2002; 1–12.
11. U.S. Department of Agriculture. *Importation of Solid Wood Packaging Material; Draft Environmental Impact Statement*; U.S. Department of Agriculture: Riverdale, MD, 2002.
12. Feng, H.; Tang, J.; Cavalier, R.P.; Plumb, O.A. Heat and mass transport in microwave drying of porous materials in a spouted bed. *AIChE Journal* **2001**, *47*, 1499–1512.
13. Salagnac, P.; Glouannec, P., Lecharpentier, D. Numerical modeling of heat and mass transfer in porous medium during combined hot air, infrared and microwaves drying. *International Journal of Heat and Mass Transfer* **2004**, *47*, 4479–4489.
14. Torres, S.S.; Jomaa, W.; Puiggal, J.R.; Avramidis, S. Multiphysics modeling of vacuum drying of wood. *Applied Mathematical Modeling* **2011**, *35*, 5006–5016.
15. Hassini, L.; Peczalski, R.; Gelet, J.L. Combined convective and microwave drying of agglomerated sand: Internal transfer modeling with the gas pressure effect. *Drying Technology* **2013**, *31*, 898–904.
16. Constant, T.; Moyne, C.; Perré, P. Drying with internal heat generation: Theoretical aspects and application to microwave heating. *AIChE Journal* **1996**, *42*(2), 359–368.
17. Antti, A.; Zhao, H.; Turner, I. An investigation of the heating of wood in an industrial microwave applicator: Theory and practice. *Drying Technology* **2000**, *18*, 1665–1676.
18. Hansson, L.; Antti, L. Modeling microwave heating and moisture redistribution in wood. *Drying Technology* **2008**, *26*, 552–559.
19. Truscott, S.L.; Turner, I.W. A heterogeneous three-dimensional computational model for wood drying. *Applied Mathematical Modeling* **2005**, *29*, 381–410.
20. Perré, P.; Turner, I.W. The use of numerical simulation as a cognitive tool for studying the microwave drying of softwood in an over-sized waveguide. *Wood Science and Technology* **1999**, *33*, 445–464.
21. Perré, P.; Turner, I.W. A 3-D version of TransPore: a comprehensive heat and mass transfer computational model for simulating the drying of porous media. *International Journal of Heat and Mass Transfer* **1999**, *42*(24), 4501–4521.
22. Rémond, R.; Passard, J.; Perré, P. The effect of temperature and moisture content on the mechanical behaviour of wood: A comprehensive model applied to drying and bending. *European Journal of Mechanics A/Solids* **2007**, *26*, 558–572.
23. Oloyede, A.; Groombridge, P. The influence of microwave heating on the mechanical properties of wood. *Journal of Materials Processing Technology* **2000**, *100*, 67–73.
24. Ouertani, S.; Koubaa, A.; Azzouz, S.; Hassini, L.; Ben Dhib, K.; Belghith, A. Vacuum contact drying kinetics of Jack pine wood and its influence on mechanical properties: Industrial applications. *Heat Mass Transfer* **2015**, *51*(7), 1029–1039.
25. ASTM. D143-94(2000) e1, *Standard Test Methods for Small Clear Specimens of Timber*; ASTM International: West Conshohocken, PA, 2007.
26. Whitaker, S. Simultaneous heat, mass, and momentum transfer in porous media: A theory of drying. *Advances in Heat Transfer* **1977**, *54*, 13.119–13.203.
27. Plumb, O.A.; Spoleck, G.A.; Olmstead, B.A. Heat and mass transfer in wood during drying. *International Journal of Heat and Mass Transfer* **1985**, *28*, 1669–1678.
28. Ben Nasrallah, S.; Perré, P. Detailed study of a model of heat and mass transfer during convective drying of porous media. *International Journal of Heat and Mass Transfer* **1988**, *31*, 957–967.
29. Perré, P.; Degiovanni, A. Simulation par volumes finis des transferts couplés en milieux poreux anisotropes: séchage du bois à basse et à haute température. *International Journal of Heat and Mass Transfer* **1990**, *33*, 2463–2478.
30. Ouelhazi, N.; Arnaud, G.; Fohr, J.P. A two-dimensional study of wood plank drying. The effect of gaseous pressure below boiling point. *Transport in Porous Media* **1992**, *7*, 39–61.
31. Turner, I.W. A two-dimensional orthotropic model for simulating wood drying processes. *Applied Mathematical Modeling* **1996**, *20*, 60–81.
32. Ni, H.; Datta, A.K.; Torrance, K.E. Moisture transport in intensive microwave heating of biomaterials: A multiphase porous media model. *International Journal of Heat and Mass Transfer* **1999**, *42*, 1501–1512.
33. Zhang, Z.; Kong, N. Nonequilibrium thermal dynamic modeling of porous medium vacuum drying process. *Mathematical Problems in Engineering* **2012**, *2012*, 1–22.
34. Donald, W.L.; Hatcher, J.D.; Sunderland, J.E. Drying of a porous medium with internal heat generation. *International Journal of Heat and Mass Transfer* **1972**, *15*, 897–905.
35. Du, G.; Siqun W.; Zhiyong, C. Microwave drying of wood strands. *Drying Technology* **2005**, *23*, 1–16.
36. Torgovnikov, G.; Vinden, P. High-intensity microwave wood modification for increasing permeability. *Forest Products Journal* **2009**, *59*, 84–92.
37. Younsi, R.; Kocaefe, D.; Poncsak, S.; Kocaefe, Y.; Gastonguay, L. CFD modeling and experimental validation of heat and mass transfer in wood poles subjected to high temperatures: A conjugate approach. *Heat and Mass Transfer* **2008**, *44*, 1497–1509.

APPENDIX A

Coefficients of liquid flux:

$$D_l^P = \left[-\overline{\rho_l}\frac{k_l k_{rl}}{\mu_l}\right];\quad D_l^T = \left[\overline{\rho_l}\frac{k_l k_{rl}}{\mu_l}\frac{\partial P_c}{\partial T}\right];\quad D_l^M = \left[\overline{\rho_l}\frac{k_l k_{rl}}{\mu_l}\frac{\partial P_c}{\partial M}\right].$$

Coefficients of vapor flux:

$$D_v^P = -\left[\overline{\rho_v^g}\frac{k.k_{rg}}{\mu_g} - D_{eff}\left(\frac{M_a M_v}{M_g RT}\right)\frac{P_v}{P_g}\right] = -\left[\overline{\rho_v^g}\frac{k.k_{rg}}{\mu_g} - D_{eff}\frac{M_a M_v P_v}{RT\left(M_a\left(P_g - P_v\right) + M_v P_v\right)}\right]$$

$$D_v^M = -\left[D_{eff}\left(\frac{M_a M_v}{M_g RT}\right)\frac{\partial P_v}{\partial M}\right] = -D_{eff}\frac{M_a M_v P_g}{RT\left(M_a\left(P_g - P_v\right) + M_v P_v\right)}\frac{\partial P_v}{\partial M}$$

$$D_v^T = -\left[D_{eff}\left(\frac{M_a M_v}{M_g RT}\right)\frac{\partial P_v}{\partial T}\right] = -D_{eff}\frac{M_a M_v P_g}{RT\left(M_a\left(P_g - P_v\right) + M_v P_v\right)}\frac{\partial P_v}{\partial T}.$$

Coefficients of dry air flux:

$$D_a^M = \left[D_{eff}\left(\frac{M_a M_v}{M_g RT}\right)\frac{\partial P_v}{\partial M}\right] = D_{eff}\frac{M_a M_v P_g}{RT\left(M_a\left(P_g - P_v\right) + M_v P_v\right)}\frac{\partial P_v}{\partial M} = -D_v^M$$

$$D_a^T = \left[D_{eff}\left(\frac{M_a M_v}{M_g RT}\right)\frac{\partial P_v}{\partial T}\right] = D_{eff}\frac{M_a M_v P_g}{RT\left(M_a\left(P_g - P_v\right) + M_v P_v\right)}\frac{\partial P_v}{\partial T} = -D_v^T$$

$$D_a^P = \left[-\overline{\rho}_a^g\frac{K_g\, k_{rg}}{\mu_g} + \left(D_{eff}\frac{M_a M_v}{M_g RT}\right)\frac{P_v}{P_g}\right] = -\overline{\rho}_a^g\frac{K_g\, k_{rg}}{\mu_g} + D_{eff}\frac{M_a M_v P_v}{RT\left(M_a\left(P_g - P_v\right) + M_v P_v\right)}.$$

Coefficients of pressure equation:

$$\gamma_1 = \left[\frac{\varepsilon M_a(1-S)}{RT}\right].\gamma_2 = \left[\frac{\varepsilon M_a(1-S)}{RT}\right]\left[\frac{\rho_s\left(P_v - P_g\right)}{\varepsilon\,\rho_l(1-S)} - \frac{\partial P_v}{\partial M}\right]$$

$$\gamma_3 = \left[\frac{\varepsilon M_a(1-S)}{RT}\right]\left[\frac{P_v - P_g}{T} - \frac{\partial P_v}{\partial T}\right],$$

where M_g is the density of the gaseous phase $M_g = \frac{M_a P_a + M_v P_v}{P_g}$ and S is the saturation.

$$S = \frac{\rho_s}{\varepsilon\,\rho_l}(M - M_{psf}).$$

APPENDIX B

Physical properties for softwood used in the simulation[21,29,30,37]

Wood properties	Value or correlation
Density of solid matrix	$\rho_s = 450$ (kg/ m^3)
Porosity	$\varepsilon = 0.67$
Specific heat of product	$C_{ps} = 1400$ (J/(kg. K))
Specific heat of liquid water	$C_{pl} = 4184$ (J/(kg. K))
Capillary pressure	$P_c(M,T) = 1.364.10^5 \quad .\sigma.(M_l + 1.2\ 10^{-4})^{-63}$
	$\sigma(T) = (77.5 - 0.185T)10^{-3} \quad$ N/m (T°C)
Mass diffusion coefficient of vapor in air	$D_{va} = 2.17.10^{-5}.(P_{atm}/P_g) \quad .(T/273.15)^{1.88}$
Gaseous diffusion coefficient	$D_{eff} = K_{rg}.\ D_{va}.\ 10^{-3}$
Bound water diffusion coefficient	$D_b^T = \exp(-9.9 - \frac{4300}{T} + 9.8\,M_b)(m^3/s)$
Thermal conductivity	$\lambda^T = 0.12 + 0.23$ M (W/(mK))
Intrinsic liquid permeability	$K_l = 10^{-15}$
Intrinsic gas permeability	$K_g = 10^{-16}$
Liquid relative permeability	$K_{rl}^T = S^3$
Gaseous relative permeability	$K_{rg}^T = 1 + (2.S - 3)(S)^2$
Sorption isotherms	$a_w = 1 - \exp(-0.76427.(M_b/M_{fsp}) - 3.6787.(M_b/M_{fsp})\text{^}2)$ if $M <= M_{fsp}$
	$a_w = 1$ if $M > M_{fsp}$
Fiber saturation point	$M_{fsp} = 0.325 - (0.001 \times (T - 273))$
Heat of vaporization	$H_{vap} = (2503 - 2.46 \times (T - 273))10^3 (J/kg)$
Loss factor	$\varepsilon'' = 1.3 + ((2.4 - 1.3)/0.2) \times (M - 0.2)$ if $(M > 0.2)$
	$\varepsilon'' = 0.2 + ((1.3 - 0.2)/0.2) \times M$ if $(M <= 0.2)$
Heat capacity	$\overline{\rho Cp} = \rho_s.(1113 + 4.85 \times T + 4185M)$
Vapor pressure saturation	$P_{vs}(T) = \exp(25.5058 - 5204.9/(T + 273.15))(P_a)$
Bound water	$M_b = \min(M_{fsp}, M)$
Free water	$M = M_b + M_l$
Heat of sorption	$H_{sorp} = 0.4H_{vap}((M_{fsp} - M_b)/M_{fsp}))^2$